Plant Stress 21 (2026) 101389

Contents lists available at ScienceDirect

Plant Stress

journal homepage: www.sciencedirect.com/journal/plant-stress

Na-salicylate and S-methylmethionine modulate stress-responsive ionomic and metabolomic pathways in Szarvasi-1 energy grass

Brigitta Müller [a], Kinga Benczúr [b], Zoltán May [c], Brigitta Tóth [d,e], Paul Lopez [a], Vitor Arcoverde Cerveira Sterner [a], Gyula Sipos [f], Csaba Gyuricza [g], Gabriella Szalai [b], Ferenc Fodor [a,*]

[a] Department of Plant Physiology and Molecular Plant Biology, ELTE Eötvös Loránd University, H-1117 Budapest, Hungary
[b] Hungarian Research Network, Centre for Agricultural Research, Agricultural Institute, Martonvásár, H-2462, Hungary
[c] Institute of Materials and Environmental Chemistry, HUN-REN Hungarian Research Network, H-1117, Budapest, Hungary
[d] Institute of Food Science, Faculty of Agricultural and Food Sciences and Environmental Management, University of Debrecen, H-4032 Debrecen, Hungary
[e] Institute of Engineering and Agricultural Sciences, University of Nyíregyháza, H-4400 Nyíregyháza, Hungary
[f] Agricultural Research and Development Institute, H-5540 Szarvas, Hungary
[g] Institute of Agronomy, Hungarian University of Agriculture and Life Sciences, H-2100, Gödöllő, Hungary

A R T I C L E I N F O

Keywords:
Drought tolerance
Biostimulants
Sodium salicylate
S-methylmethionine
Elymus elongatus
Metabolomic profiling

A B S T R A C T

Drought is a major constraint on agricultural productivity and developing sustainable strategies to enhance crop resilience is critical under climate change. This study investigated the effects of foliar-applied sodium salicylate (NaSA) and S-methylmethionine (SMM) on the physiology, metabolism, and ion homeostasis of Szarvasi-1 energy grass (*Thinopyrum obtusiflorum cv. Szarvasi-1*) under field drought conditions. Treatments were applied in small- and large-scale field experiments over two consecutive years characterized by varying drought intensities. Neither NaSA nor SMM significantly altered biomass accumulation, leaf water content, or chlorophyll levels. However, both treatments improved photosynthetic performance, particularly in small-scale experiments, enhancing CO_2 assimilation, transpiration, and photosystem II efficiency. Enzyme assays revealed that NaSA and SMM modulated the antioxidant defence system by increasing superoxide dismutase, peroxidase, and glutathione reductase activities, while catalase and ascorbate peroxidase activities decreased. Elemental analysis showed treatment-dependent adjustments in potassium and sodium levels, resulting in elevated K:Na ratios, which support osmotic regulation under drought. Metabolomic profiling indicated that SMM predominantly enhanced lignin and phenolic biosynthesis and sugar-mediated osmotic adjustment, whereas NaSA triggered broader metabolic reprogramming, including amino acid metabolism, secondary metabolites, and photorespiratory pathways. Principal component analysis confirmed distinct metabolic responses to each biostimulant, highlighting complementary strategies for drought adaptation. Overall, SMM and NaSA improve physiological and biochemical drought tolerance in Szarvasi-1, providing insights for the use of natural biostimulants to enhance stress resilience in biomass crops.

1. Introduction

Drought is one of the most pervasive global constraints and considering the escalating trend of climate change and global warming, its adverse impacts are expected to intensify in numerous agriculturally significant regions (Dietz et al., 2021). Drought stress has shown notable effects on the morphological, physiological, biochemical, and molecular characteristics of plants, resulting in a decline in their photosynthetic capacity (reviewed in Seleiman et al., 2021). In response to water scarcity, plants developed diverse and complex resistance mechanisms (reviewed in Gupta et al., 2020; Batool et al., 2022). Increased production of reactive oxygen species (ROS) in cellular compartments like chloroplasts and mitochondria is an inevitable consequence of drought stress. Enhanced ROS generation induced by drought stress, however, kept under tight control by a highly adaptable and cooperative antioxidant system that effectively regulates intracellular ROS levels and

* Corresponding author at: Department of Plant Physiology and Molecular Plant Biology, ELTE Eötvös Loránd University, Pázmány Péter lane 1/c, 1117 Budapest, Hungary.
E-mail address: ferenc.fodor@ttk.elte.hu (F. Fodor).

https://doi.org/10.1016/j.stress.2026.101389
Received 1 February 2026; Received in revised form 30 March 2026; Accepted 19 April 2026
Available online 20 April 2026

maintains the cell's redox balance. Moreover, ROS production during stressful conditions serves as a warning signal, activating the defence mechanisms or adaptation processes. When faced with drought, plants primarily respond by closing their stomata to minimize water loss via transpiration (Li et al., 2020). This closure leads to decreased photosynthesis rates due to reduced CO_2 concentration within the leaves, resulting in diminished consumption of NADPH and ATP. Consequently, the regeneration of electron acceptors also declines, leading to an overproduction of ROS (Shemi et al., 2021). In addition to the decline in photosynthetic capacity and the accumulation of ROS, a decrease in the relative water content (RWC) is commonly observed as a symptom of drought stress in a variety of plant species (Badr and Brüggemann, 2020). Leaf relative water content reflects the balance between water uptake by leaf tissue and the rate of transpiration. When water levels drop, plant cells lose turgor pressure, resulting in cell damage, wilting, and impaired plant growth. Consequently, assessing relative water content is crucial for evaluating drought stress severity. Plant shoot and root growth is generally reduced when soil water supply is limited (de Araújo Silva et al., 2021). Water deficiency leads to a severe decline in biomass production of crop plants probably by disrupting leaf gas exchange due to stomatal closure (Zahra et al., 2023).

Plants respond to water deficit through various strategies including reduction of transpiration loss by altering stomatal conductance and distribution as well as by the enhancement of water absorption from well-established root systems (Bashir et al., 2021). Furthermore, mechanisms such as osmotic adjustment, antioxidant defence systems, accumulation of cell-protective metabolites, along with an increase in the root-to-shoot ratio, are common strategies enabling plants to withstand the detrimental effects of drought stress (Bandurska, 2022). Osmoregulation in plants facing low water potential depends on the production and buildup of osmoprotectants or osmolytes, which include soluble proteins, sugars, sugar alcohols, betaines, and amino acids such as proline and phytohormones like indole acetic acid (reviewed in Ozturk et al., 2021). The antioxidant defence system plays a crucial role in regulating the accumulation of reactive oxygen species (ROS) and maintaining cellular redox balance. Enzymatic elements consist of superoxide dismutase (SOD), which serves as the primary defence mechanism by converting superoxide anions into hydrogen peroxide (H_2O_2). Subsequently, the generated H_2O_2 can be further neutralized by catalase (CAT) located in peroxisomes or ascorbate peroxidase (APX), which is prevalent throughout plant cells and participates in the ascorbate-glutathione (Asa-gsh) pathway. In addition to the enzymatic protection, ascorbate stands out as a pivotal antioxidant molecule in plant tissues, capable of directly scavenging ROS while also playing a vital role in the Asa-gsh cycle. Enhanced antioxidant mechanisms have been linked to improved tolerance to drought stress (Lourkisti et al., 2022).

Several methods exist for mitigating the impact of drought on agriculture, including employing tolerant varieties (such as those with early maturation), implementing soil conservation practices, establishing efficient irrigation systems, applying mulch for soil conservation, conducting in vitro selection to screen for drought-tolerant varieties. Developing drought-resistant crops *via* metabolic engineering methods – increasing the amount of osmoprotectants and antioxidants – offers an alternative viable approach to protect plants from drought stress. Applying exogenous osmoprotectants like glycine betaine or salicylic acid (SA) to enhance plant defences against drought stress is increasingly becoming a prevalent strategy in agriculture (Pamungkas and Farid, 2022). Given the urgent and increasing requirement in the twenty-first century to establish sustainable methods for ensuring crop productivity at a low cost and with reduced chemical inputs, there has been a growing demand in recent years for natural, biologically active substances that can enhance the nutritional and agronomic characteristics of crucial food and feed crops in agriculture (Yadav et al., 2021). Replacing synthetic chemicals by natural secondary metabolites could be a favourable option from both economic and environmental perspectives. SA and S-methylmethionine (SMM) are promising compounds, which has been proved to play a role in abiotic and biotic stress response mechanisms (Song et al., 2023; Yang et al., 2023).

SA, also known as ortho-hydroxybenzoic acid, is a member of the plant phenolic group, characterized by the presence of a benzoic acid with a hydroxyl group located at the ortho position. SA can be found in various plant species at a wide range of endogenous levels (Klessig et al., 2016). However, its role has only been recognised in the last few decades, and the exact mode of action is still not fully understood. The primary roles of SA in mitigating drought stress include: stimulating seedling growth, enhancing plant antioxidant capacity, maintaining plant water balance, promoting the activation of stress-related genes in plants, and regulating plant physiological metabolism (reviewed in Mohammed et al., 2020; Song et al., 2023). Foliar application of plant growth regulators, micronutrients, or osmoprotectants to enhance drought tolerance in plants has received increased attention. Most studies in this field have focused on the effects of SA under drought stress conditions, particularly in maize (Shemi et al., 2021), rice (Sohag et al., 2020) and other crops such as wheat (Khalvandi et al., 2021) and barley (Pirasteh-Anosheh et al., 2022). Although the exact mechanisms and pathways through which SA enhances stress tolerance are not fully understood, recent studies have explored how SA cooperates with various small molecules to regulate biotic and abiotic stress responses (Xin et al., 2024).

The influence of applying SA on plants under abiotic stress may exhibit diverse effects, potentially leading to either harmful consequences or beneficial protective outcomes. The result depends on factors such as the plant species, the concentration of SA applied, and the method of application. In addition, various forms of SA may result in different effects on plants via distinct mechanisms. Recently, it was clearly demonstrated that different forms of SA may induce very diverse defence mechanisms in maize. While SA caused a dramatic increase in catalase (CAT) activity, sodium-salicylate (NaSA) triggered the CAT activity moderately. In the same study, NaSA promoted the glutathione (GSH)-related antioxidant enzymes, while the other antioxidant enzymes have been influenced by SA (Gondor et al., 2016). However, the type of SA, used in a study, is frequently left unspecified. Only a limited number of papers referencing SA treatment provide clarity on whether the acidic form of SA or NaSA was applied. In this study, we applied exogenously added NaSA by spraying it to allow penetration into both the soil and the plant shoot and leaves.

Amino acids, serving as natural enhancers for plant growth, are also widely employed to increase crop productivity (Maqsood et al., 2022). SMM is a non-proteinogenic amino acid synthesized from methionine and S-adenosylmethionine. SMM is actively involved in the cellular methylation processes having a crucial function in sulphur transportation and storage. Beyond its significance in sulphur metabolism, SMM directly or indirectly contributes to the stress tolerance of plants (reviewed in Bouranis and Chorianopoulou, 2023). SMM plays a crucial role in the synthesis of sulphopropionates, serving as osmoprotectants, and polyamines, contributing significantly to plant resilience against drought stress (Ludmerszki et al., 2014). SMM has been proved to mitigate the adverse effects of drought stress by promoting dimethyl sulphopropionate production, which is an osmoprotectant (Ogawa and Mitsuya, 2012) and by increasing the biosynthesis of polyamines (reviewed in Singh et al., 2015). However, foliar SMM treatment and its effect on the plant metabolism and productivity have not been investigated yet.

Despite the numerous promising outcomes attained using SA and SMM to enhance crop stress tolerance, several considerations must be acknowledged. Primarily, most of the research has been conducted in controlled environmental settings, typically involving the alteration of only a limited number of parameters. In field conditions, particularly under extreme climates, the results may vary significantly. Here, NaSA and SMM treatment has been conducted both in small scale field experiment and in high-scale agricultural field conditions using a tall wheatgrass cultivar, Szarvasi-1 energy grass ((*Thinopyrum obtusiflorum* cv. Szarvasi-1, *syn. Elymus elongatus* subsp. *ponticus, Agropyron elongatum, Elytrigia elongata; Poaceae, Triticeae)* as a model plant.

Szarvasi-1 is a perennial grass developed in Hungary specifically for biomass production on marginal lands. Its biomass has a high value as a forage but due to its high fiber content it is a good raw material in industry and ultimately for energy production in biogas plants and as hay or pellet for combustion. Due to its deep root system, adaptability to poor soils, and low input requirements, it is considered a sustainable option for long-term biomass cultivation under Central European conditions (Csete et al., 2011; Sipos et al., 2013). Szarvasi-1 can sustain high-yielding perennial populations for over a decade and under favourable precipitation it can yield 10–25 t ha^{-1} of dry matter annually, although yields decline significantly under drought or nutrient limitation (Csete et al., 2011; Ciria et al., 2020). One of its most remarkable features is its tolerance to abiotic stresses, including drought, salinity, and nutrient deficiency, which allows its cultivation in semi-arid or degraded environments (Rév et al., 2017; Rana et al., 2025; Sterner et al., 2024). Nevertheless, water limitation remains the major factor constraining biomass accumulation, particularly in dry growing. These characteristics position Szarvasi-1 not only as a promising biomass crop but also as a valuable model species for investigating physiological responses to water deficit and for evaluating agronomic practices or external inputs, such as biostimulants, that may enhance drought resilience. We hypothesised that SMM and NaSA might influence the stress tolerance, nutrient uptake and allocation, metabolite patterns and biomass yield of Szarvasi-1 energy grass under drought stress. We made an attempt to reveal the interconnections of these using combined chemical and plant physiological approaches.

2. Materials and methods

2.1. Experimental sites and soil characteristics

The SMM and NaSA treatments were applied under field conditions at two different locations in Hungary. One experimental site was located in Göd, where smaller plots (0.2 m^2 quadrats) were established (small-scale experiment), while the other was in Szarvas, where larger plots (1 m^2 quadrats) were set up under conventional open-field, ploughed conditions (large-scale experiment). The soil characteristics of the two sites derived from analysing average samples in the upper 0 – 30 cm layer is provided in Supplementary Table S1.

2.2. Plant material, foliar treatments and biomass yield assessment

Szarvasi-1 energy grass seeds have been planted (2 cm deep) in the previously prepared soil surface in September 2018. The grass was mowed twice next year in July and November. The plantations were 2 years-old in 2020 when the study was started. SMM and NaSA treatment was scheduled in spring during the rapid elongation phase of the energy grass. The first treatment was made between April 24 and May 06 while the second one between May 18 and 27. 0.5 dm^3 m^{-2} of 0.05 mM SMM and NaSA solution was sprayed onto plant foliage containing 0.025% nonit (Agrokémia Sellye Plc.) as a surfactant. Control group was treated with distilled water (also containing nonit) in the same amount. In the small-scale experiments, the control, SMM, and NaSA treatments were applied to seven quadrates. The space between the quadrates was 20 cm. In the large-scale experiments, five randomly located quadrates marked in a previously established agricultural plantation were treated similarly, and each quadrate was placed 1 m distance from the neighbouring ones on each side. The treatments were made in a completely randomised block design. Aerial parts of the plants of the whole quadrates were harvested at the beginning of July to measure biomass yield.

2.3. Meteorological data and sampling for drought stress experimentation

The experiments conducted in 2020 and 2021, aimed to assess the resistance to drought in the two locations, Göd and Szarvas. Both years were characterized by varying drought conditions, with 2021 being notably drier than 2020 at both sites (Supplementary Fig. S1). In 2020, Göd experienced a prolonged period of severe drought, particularly before June, when the sampling occurred. During this time, only 91.5 mm of precipitation was recorded from January to May (531.5 mm whole year), which is considered very low in Hungary, especially compared to other regions where rainfall typically ranges between 600 and 800 mm annually. Such low precipitation is characteristic of drier areas, like the southern and eastern parts of the Great Plain, where drought stress can significantly affect plants. However, 2021 was marked by multiple severe drought periods that persisted throughout the study period, lasting until harvest. Despite moderate precipitation levels of 161 mm from January to May (442.5 mm whole year), the drought conditions in 2021 were more prolonged and intense compared to the previous year. In Szarvas, the year 2020 received a total of 700 mm of precipitation, with severe drought conditions observed only one week before the sampling. However, Szarvas faced a more severe drought throughout 2021, which contributed to the challenging environmental conditions at both sites.

In both years, treatments were applied at the end of April, and most sampling (metabolomics, element analysis, and enzyme activity assays) was conducted one month later, at the end of May, corresponding to the vegetative growth phase. This stage represents the most intensive growth period of energy grass under optimal conditions, although, in our study, growth was likely limited by water availability. Accordingly, samples for metabolomics, element analysis, and enzyme activity measurements were collected exclusively from Göd during this defined developmental stage and under distinct drought conditions. Photosynthetic parameters in Göd were measured concurrently with sampling. In contrast, photosynthetic measurements in Szarvas were conducted later, shortly before harvest, representing a more advanced developmental stage at the transition between late vegetative and early reproductive phases. This later assessment reflects plant performance under prolonged drought stress rather than early stress responses. Biomass production was assessed at harvest at both sites. The considerable variability in precipitation observed at both sites emphasizes the need to investigate drought stress effects under diverse meteorological conditions. Notably, the 2021 drought was more pronounced and extended at both Göd and Szarvas, providing a valuable opportunity to study the resilience of plants and efficiency of the treatments under sustained drought stress.

2.4. Determination of water content

Fresh weight was measured directly after harvesting the aerial part of the plants. Fresh weight of five-seven individual plants from each quadrate was measured separately and the dry weight of them was used to determine the water content.

2.5. Measurements of transpiration and photosynthetic performance

Photosynthetic activity and transpiration were measured as previously described by Müller et al. (2022), using an LI-6800F portable photosynthesis system (LICOR Biosciences, Lincoln, NE, USA).

2.6. Determination of the relative chlorophyll content

A hand-help SPAD-502+ (Minolta Camera Co., Osaka, Japan) was used to estimate chlorophyll content. This instrument has a 0.06 cm^2 measurement area and calculates an index in SPAD units. After cleaning surface dust from the selected youngest fully developed leaves, on each leaf, five SPAD readings were taken from each quadrate. The five readings were averaged to produce a single observation value for each quadrat. In the small-scale experiment, five quadrats were randomly selected, whereas in the large-scale experiment at Szarvas, measurements were taken from all five established quadrats. While recording SPAD readings, care was taken to ensure that SPAD meter sensor fully covered the leaf lamina and that interference from midribs was avoided.

2.7. Determination of superoxide dismutase, class III and ascorbate peroxidase activity

Around 100 mg of fresh plant material was processed as previously described by Müller et al. (2022), including homogenization, solubilization, and protein extraction. Protein complexes were resolved by PAGE using 10–18% gradient gels according to Laemmli (1970). Enzymatic activities of superoxide dismutase (SOD; EC 1.15.1.1) and class III peroxidases (POD; EC 1.11.1.7) were determined and visualized as described in Müller et al. (2022), following the protocols of Giannapolitis (1977) and Solórzano et al. (2020), respectively. Total activities were quantified by densitometric analysis of the stained bands.

2.8. Glutathione reductase, ascorbate peroxidase, catalase and guiacol peroxidase activity

Enzyme extracts were prepared as previously described by Müller et al. (2022). Protein concentrations were determined using the method of Bradford (1976), with bovine serum albumin as the standard, and absorbance readings were taken on a UV–VIS spectrophotometer (Shimadzu, Japan).

Glutathione reductase (GR; EC 1.8.1.7) activity was measured as described in Müller et al. (2022), following the method of Smith et al. (1988).

The activity of ascorbate peroxidase (APX; EC 1.11.1.11) was determined according to Nakano and Asada (1981) by monitoring the decrease in absorbance at 290 nm, which corresponds to the H_2O_2-dependent oxidation of ascorbate. The enzyme activity was calculated based on the decrease in ascorbate concentration (monitored at 290 nm), which reflects H_2O_2-dependent oxidation, using an extinction coefficient of $\varepsilon = 2.8$ mM^{-1} cm^{-1}. The reaction mixture (750 μL) contained 200 mM Tris buffer (pH 7.8), 1 mM H_2O_2, 0.5 mM ascorbic acid, 0.1 μM EDTA, and 50 μL of enzyme extract.

Catalase (CAT; EC 1.11.1.6) activity was measured as described in Müller et al. (2022), following the method of Aebi (1984).

Guaiacol peroxidase (GPOX; EC 1.11.1.7) activity was measured following the method of Konieczny et al. (2014), by monitoring the increase in absorbance at 470 nm, resulting from the oxidation of guaiacol. The total reaction volume was 750 μL. The reaction mixture consisted of 100 mM phosphate buffer (pH 7.0) with 4.375 mM guaiacol, 0.1 mM EDTA, and 15 mM H_2O_2 with the reaction being initiated by the addition of 18.75 μL enzyme extract. The phosphate buffer (1 M, pH 7.0) was prepared by combining 39 mL of 2 M NaH_2PO_4, 61 mL of 2 M Na_2HPO_4, and 100 mL of deionized water. The enzyme activity was calculated based on the amount of guaiacol oxidized (tetraguaiacol) during the reaction, using an extinction coefficient of $\varepsilon = 26.6$ mM^{-1} cm^{-1} at 470 nm.

2.9. Metabolite profiles

Metabolic profile of the plants treated with different biostimulants such as SMM and NaSA was analysed only in small-scale field conditions due to the constraints related to sampling for preserving the actual metabolite pattern of the leaves. Differential metabolites were discussed by comparing control and treated plants in leaves responding to drought stress. A total of 32 compounds – out of the 64 metabolites measured – were consistently detected and quantified in samples collected over two years. These included 16 amino acids (valine, alanine, glycine, proline, leucine, isoleucine, serine, threonine, methionine, aspartic acid, glutamic acid, asparagine, 5-oxoproline, phenylalanine, tyrosine, alanylglycine (ISTD)); 11 organic acids (oxalic acid, succinic acid, fumaric acid, malic acid, aconitic acid, shikimic acid, SA, caffeic acid, glycolic acid (ISTD), malonic acid (ISTD), glyceric acid (ISTD)); 3 sugars and sugar derivatives (glucose, fructose, ascorbic acid (ISTD)); and 2 nucleotides and cofactors (adenine (ISTD), niacin/B3 vitamin (ISTD)), which were identified in each polar extract. Internal standard (ISTD) was used for certain compounds, making the obtained values interpretable only relative to each other. For the remaining compounds, absolute quantification was performed. This approach enables relative comparisons for ISTD-based compounds' concentrations, ensuring consistent detection despite potential extraction or instrument sensitivity variability. Only metabolites measurable in at least one year were included; those not measurable in both years were excluded. Metabolites below the detection limit or exhibiting excessive variability were also excluded, and these are listed in the supplementary material (Supplementary Table S2).

Sample preparation was made based on the method of Gondor et al. (2021) with some modifications. Samples were extracted first with 60% and then 90% of methanol. Ribitol (Merck-Sigma group, Darmstadt, Germany) as internal standard was added, which is a stable component. After centrifugation the collected supernatants were evaporated to dryness and used for two-step derivatisation with methoxyamine hydrochloride dissolved pyridine (Merck-Sigma group, Darmstadt, Germany) and N-trimethylsilyl-N-methyl trifluoroacetamide (Merck-Sigma group, Darmstadt, Germany). The samples were transferred and injected into LECO Pegasus 2D GCxGC TOFMS (LECO Corporate, St Joseph, Michigan, USA). Rxi-5MS (30 m, 0,25 mm ID, 0,25 μm) as a primary, while Rxi-17Sil MS (1.5 m, 0,15 mm ID, 0,15 μm) as a secondary column were used and the carrier gas was He (1 ml min^{-1}). The thermal program started at 70 °C for 3 mins and increased by 7 °C min^{-1} to 320 °C and kept it for 5 mins. The identification of compounds is based on Kovats retention index, NIST Mass Spectral Search Program (InChI Library v 1.05), Leco-Fiehn Lib and analytical standards (Merck-Sigma group, Darmstadt, Germany). The unit of compounds is μg g^{-1} FW except which are marked with "ISTD", because these compounds have relative amount only. The evaluation was carried out using LECO ChromaTOF 4.72 software (LECO Corporate, St Joseph, Michigan, USA).

2.10. Determination of element concentration

The total aboveground material of 3 plants was collected separately at harvest. Plant samples were processed for ion content analysis as described in Müller et al. (2022). Briefly, samples were digested in concentrated HNO_3 and subsequently analysed by ICP-OES (Spectro Genesis, SPECTRO, Freital, Germany) with axial plasma viewing. For the calibration of the instrument, a multielement standard (for 33 elements) was used (Loba Chemie Product code: I166N, Loba Chemie PVT, Mumbai, India).

2.11. Statistical analysis

Data were presented as means with standard deviations. Water content measurements and biomass determination in both the small-scale (Göd) and the large-scale (Szarvas) field experiment were based on samples from at least 5 (up to 7) randomly selected quadrates. For chlorophyll content, 4–5 SPAD readings were taken from a representative plant chosen from at least 5 random quadrates. Photosynthetic parameters and enzymatic activities were averaged from 3 measurements, with 3 technical replicates for enzyme assays. Metabolomic analysis used the average of 4 biological replicates, while elemental analysis was based on 5 biological replicates, both conducted only for the Göd samples. For the metabolomic and elemental data, heatmaps were generated to visualize relative increases or decreases compared to untreated control plants. Statistically significant differences are indicated by asterisks (*, **, ***) corresponding to $p < 0.05$, 0.01, or 0.001, respectively. Principal Component Analysis (PCA) was additionally performed on the metabolomic datasets to evaluate overall patterns of variation among treatments and sampling years. Statistical analysis was performed with GraphPad software, using one-way ANOVA to determine the data homogeneity followed by Tukey's post-hoc test. Statistically significant differences ($p < 0.05$) are indicated by lowercase letters.

3. Results

3.1. Effect of SMM and NaSA on the biomass yield and physiological parameters of Szarvasi-1 energy grass under drought stress

Neither SMM nor NaSA treatments caused a significant change in total biomass accumulation compared to the control (non-treated plants) in either experimental site (Fig. 1A, B). An interesting observation was that, despite the second year being significantly drier, biomass production increased in the small-scale experiment, independent of the treatments. However, no such increase was observed at the large-scale experimental site, where the conditions were similar.

Neither the SMM nor NaSA treatments caused a significant change in water content of the plants (Fig. 2A, B). The impact of SMM and NaSA treatments on transpiration intensity and CO_2 assimilation was observed in all treatments, across all experimental setups and in both years (Fig. 3A-D). However, significant changes were only measured in the first year and only in the small-scale field experiment (Fig. 3A, C). In this case, transpiration intensity was significantly increased only by NaSA, while CO_2 assimilation was significantly enhanced by both treatments.

In the first year of the small-scale experiment, the maximum quantum efficiency of PSII (Fv/Fm) was significantly increased by NaSA whereas in the second year both NaSA and SMM had a significant effect in both small-scale and large-scale experiments (Fig. 4A, B). The actual quantum efficiency of PSII (ΦPSII) was clearly enhanced by both treatments in the small-scale experiment along with a decrease in the non-photochemical quenching (NPQ) in the first year (Fig. 4C, E). However, in the second year, this effect did not persist. In the large-scale experiment, only the SMM treatment induced considerable changes (Fig. 4D, F).

Relative chlorophyll content was only measured in the second year, but neither SMM nor NaSA treatments induced any significant changes (Fig. 5). However, in line with the biomass production and relative water content, relative chlorophyll content was higher in the small-scale compared to the large-scale experiment.

3.2. Oxidative stress and antioxidative defence

Enzyme activity assays were conducted to evaluate whether biostimulant treatments influence the antioxidant defence mechanisms of Szarvasi-1 energy grass under drought stress (Fig. 6). Due to methodological constraints, these measurements were limited to the small-scale field experiments. Both SMM and NaSA treatments induced notable changes in antioxidant enzyme activities, showing similar tendencies across both experimental years. In NaSA-treated plants, SOD, POD, and GR activities were significantly enhanced, while APX and GPOX activities decreased, accompanied by a declining trend in CAT activity. Similarly, SMM treatment led to increased SOD, POD, and GR activity, whereas APX, CAT, and GPOX activities were reduced compared to untreated controls.

3.3. Element composition

In the first year of the experiment, both the SMM and NaSA treatments markedly increased the potassium (K) content in the youngest fully developed leaves of Szarvasi-1 energy grass compared to the untreated control (control: 9260.6 ± 1430.7; SMM: 21,980.7 ± 2094.2; NaSA: 22,295.6 ± 2486.8 mg kg^{-1} DW), while no significant changes were detected in sodium (Na) levels. In contrast, during the second year, the K content did not differ significantly between treated and untreated plants. Instead, the elevated K:Na ratio observed in SMM- and NaSA-treated plants was primarily due to a reduction in Na levels (control: 2654.1 ± 190.1; SMM: 1774.3 ± 651.2; NaSA: 1513.5 ± 859.6 mg kg^{-1} DW). It is also noteworthy that the K:Na ratio increased in the control plants from the first to the second year (from 3.6 ± 0.5 to 12.6 ± 0.3), indicating an overall shift in ion homeostasis under more severe drought conditions, even in the absence of biostimulant treatments. Nevertheless, the SMM and NaSA treatments further enhanced this shift, resulting in significantly higher K:Na ratios in both experimental years (Fig. 7). Exogenous application of SMM and NaSA led to a significant reduction in strontium (Sr) accumulation in treated plants during the first year of the experiment, whereas no notable differences were detected in the second year. The concentrations of other examined macro- and micronutrients remained largely unaffected by the treatments (Fig. S2, Table S3).

3.4. Metabolite composition

The metabolite content of the youngest fully developed leaves was measured during the post-treatment period, for both treatments and in both years (Fig. 8). The applied SMM evidently resulted in a notable

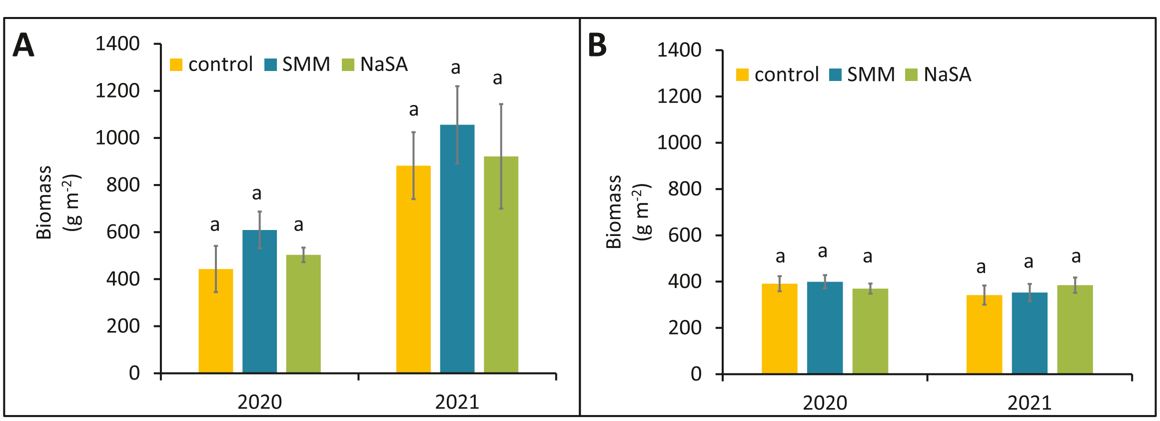

Fig. 1. Aboveground dry biomass accumulation as affected by the SMM and NaSA treatments in the small-scale experiment (in Göd) (A) and the large-scale experiment (in Szarvas) (B) conducted on Szarvasi-1 energy grass plantations in 2020 and 2021. To compare differences among the treatments, one-way ANOVA was performed with Tukey-Kramer multiple comparisons post hoc test. Same lowercase letters indicate no significant difference among the treatments ($p < 0.05$, $n = 5–7$). Error bars represent SD values. Statistical analyses were conducted separately for the small-scale and large-scale experiments and each year.

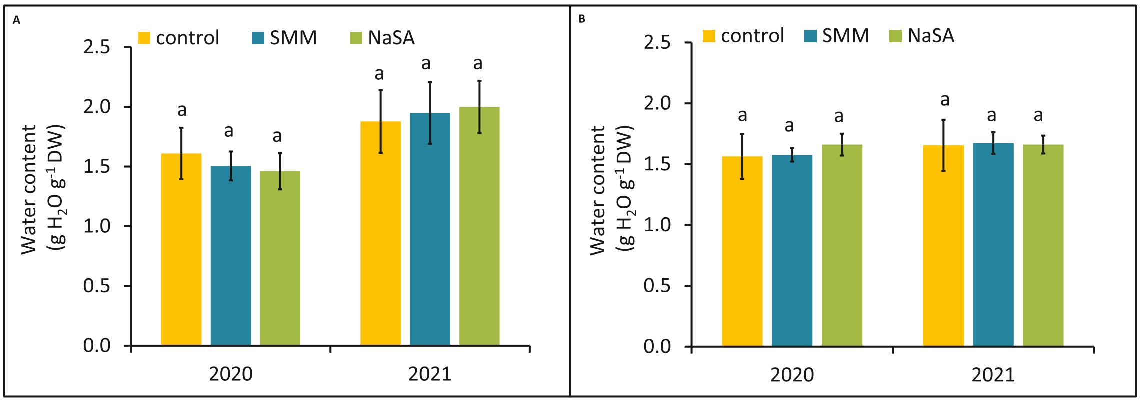

Fig. 2. Shoot water content as affected by the SMM and NaSA treatments in the small-scale experiment (in Göd) (A) and the large-scale experiment (in Szarvas) (B) conducted on Szarvasi-1 energy grass plantations in 2020 and 2021. To compare differences among the treatments, one-way ANOVA was performed with Tukey-Kramer multiple comparisons post hoc test. Same lowercase letters indicate no significant difference among the treatments ($p < 0.05$, $n = 5–7$). Error bars represent SD values. Statistical analyses were conducted separately for the small-scale and large-scale experiments and each year.

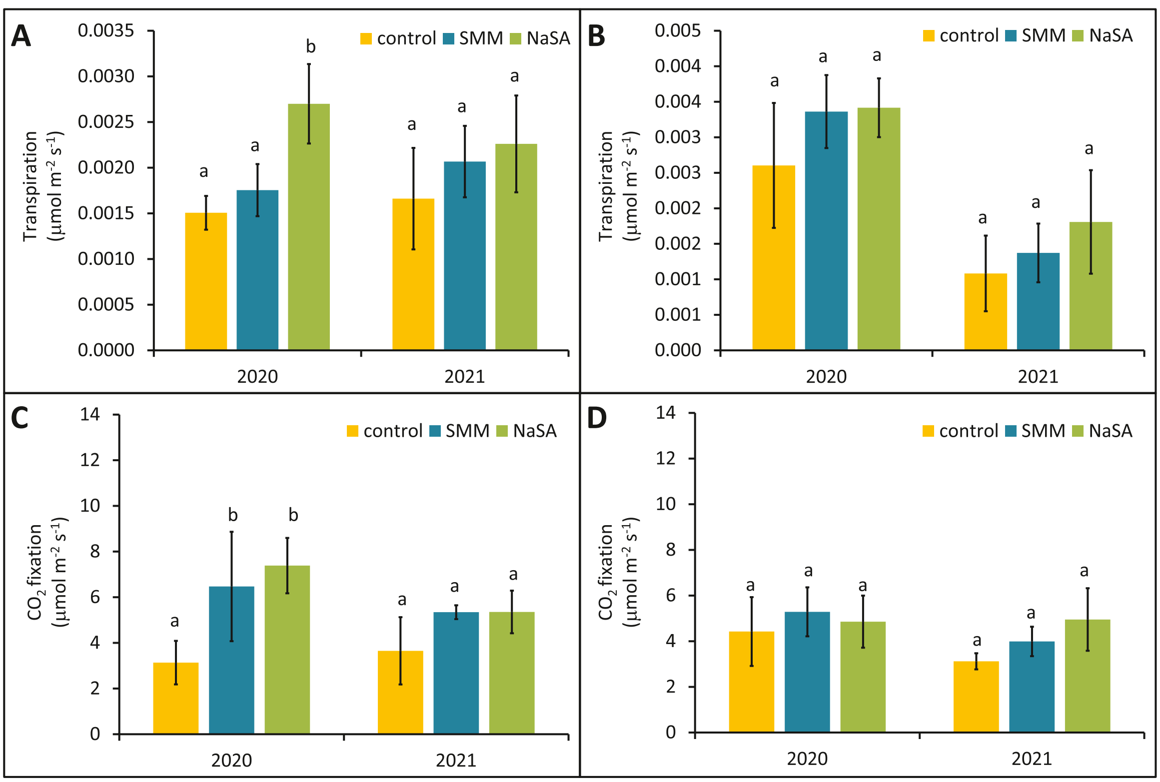

Fig. 3. Transpiration rate and CO_2 assimilation recorded in the youngest fully developed leaves as affected by SMM and NaSA treatments in the small-scale experiment (in Göd) (A, C) and the large-scale experiment (in Szarvas) (B, D) conducted on Szarvasi-1 energy grass plantations in 2020 and 2021. To compare differences among the treatments, one-way ANOVA was performed with Tukey-Kramer multiple comparisons post hoc test. Different lowercase letters indicate significant difference among the treatments ($p < 0.05$, $n = 4–6$). Error bars represent SD values. Statistical analyses were conducted separately for the small-scale and large-scale experiments and each year.

boost in the levels of oxalic acid, as well as sugars such as fructose and glucose, exhibiting an upward trend without statistically significant variance in L-methionine concentrations. However, notable reduction in the amount of various amino acids, including L-valine, L-alanine, L-serine, leucine, L-aspartic acid, L-tyrosine, phenylalanine and glycine as well as an organic acid, glyceric acid was caused in SMM treated plants. Additionally, a decreasing trend was observed in the levels of L-proline, L-isoleucine, and L-threonine, albeit not statistically significant. Also, organic acid compounds such as ascorbic acid, aconitic acid and malonic acid had a remarkable decline in SMM treated energy grass. The foliar application of NaSA yielded a noteworthy and markedly elevated concentration of oxalic acid and L-methionine, alongside increased levels of L-5-oxoproline and L-threonine. Moreover, the amount of sugars, including fructose and glucose was increased, while caffeic acid and glycolic acid content were also notably elevated in energy grass treated with NaSA. The concentration of amino acids, notably L-valine, L-alanine, glycine was decreased, with extremely significant drop observed in the levels of malonic acid, niacin, glyceric acid, alanylglycine, adenine, and ascorbic acid.

The PCA analysis revealed distinct metabolic patterns between control and treated plants, with notable differences between the first and second years (Fig. 9A, B). In the first year, SMM treatment had a

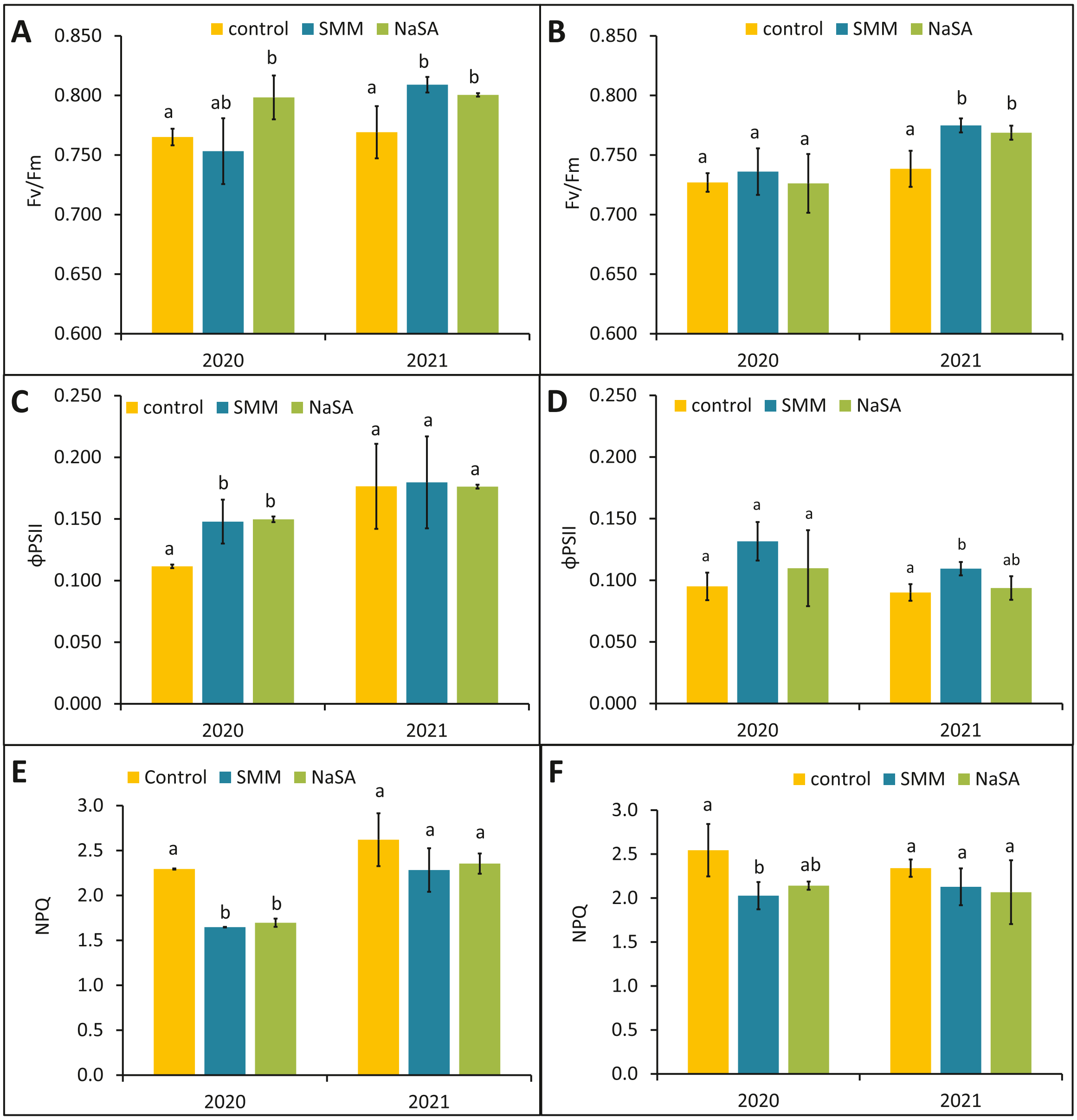

Fig. 4. Status of the photosynthetic apparatus recorded in the youngest fully developed leaves as affected by SMM and NaSA treatments in the small-scale experiment (in Göd) (A, C) and the large-scale experiment (in Szarvas) (B, D) conducted on Szarvasi-1 energy grass plantations in 2020 and 2021. To compare differences among the treatments, one-way ANOVA was performed with Tukey-Kramer multiple comparisons post hoc test. Different lowercase letters indicate significant difference among the treatments ($p < 0.05$, $n = 3–5$). Error bars represent SD values. Statistical analyses were conducted separately for the small-scale and large-scale experiments and each year. (Maximal (Fv/Fm) and the actual (ΦPSII) quantum efficiency of photosystem II reaction centres and the value of non-photochemical quenching (NPQ)).

moderate effect, primarily affecting metabolites such as shikimic acid. However, in the second year, the separation between SMM-treated and control groups was more pronounced along PC2, indicating that the metabolic changes in the SMM treated plants (group A) were more strongly represented by this component. The most significant shifts in metabolites included shikimic acid, glyceric acid, phenylalanine, L-tyrosine, malic acid, and SA.

For NaSA treatment (group B), the first year showed a stronger impact on metabolite profiles, with significant deviations along the PC1 axis. Metabolites such as L-5-oxoproline, L-methionine, L-isoleucine, L-threonine, caffeic acid, and glycolic acid exhibited high positive PC1 coefficients. In the second year, NaSA treatment still induced noticeable metabolic shifts, but the pattern shifted towards the PC2 axis, particularly affecting oxalic acid, L-5-oxoproline, and fumaric acid.

4. Discussion

Foliar applications of the biostimulants SMM and NaSA were carried out in the second and third year after sowing to investigate their effects on metabolism and antioxidant defence mechanisms in Szarvasi-1 energy grass during a two-year study. Although biomass accumulation, leaf relative water content, and chlorophyll levels remained largely unchanged, a clear improvement in photosynthetic performance was observed, particularly in the small-scale experiments. This suggests that the energy and carbon produced through photosynthesis were redirected toward drought-defence mechanisms, such as antioxidant enzyme activity or the synthesis of protective metabolites, rather than growth. As noted by Han et al. (2023), SA-induced responses often involve a reallocation of energy toward defence at the expense of biomass production. The salicylate analogue NaSA may enhance photosynthetic

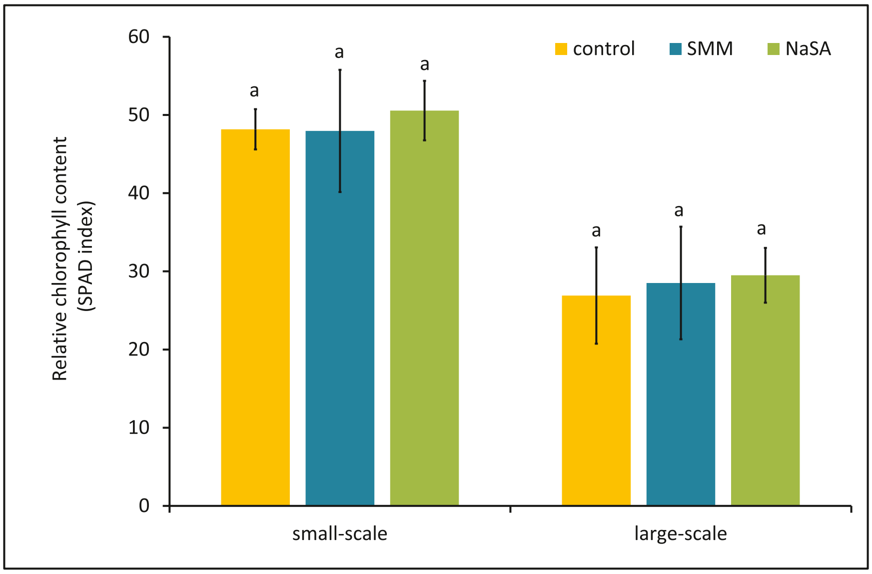

Fig. 5. Relative chlorophyll content (SPAD index) as affected by the SMM and NaSA treatments in the small-scale experiment (in Göd) and large-scale experiment (in Szarvas) conducted on Szarvasi-1 energy grass plantations in 2021. To compare differences among the treatments, one-way ANOVA was performed with Tukey-Kramer multiple comparisons post hoc test. Same lowercase letters indicate no significant difference among the treatments ($p < 0.05$, $n = 20$–25). Error bars represent SD values. Statistical analyses were conducted separately for the small-scale and large-scale experiments.

efficiency under drought by modulating stomatal conductance and improving water use efficiency, thereby maintaining CO_2 uptake and photochemical activity (Fariduddin et al., 2003; Khan et al., 2015), however, this increased photosynthetic capacity does not necessarily translate into greater biomass accumulation. Under water deficit, growth processes are frequently limited by sink capacity rather than carbon assimilation (Rodrigues et al., 2019). Consequently, the additional assimilates produced might be redirected towards stress acclimation processes, including osmoprotection, antioxidant defence, and maintenance of cellular integrity, rather than growth (Pallas et al., 2013). In addition, salicylate signalling has been linked to chloroplast membrane stabilization and the upregulation of genes encoding components of the photosynthetic electron transport chain, supporting sustained photosynthesis during stress (Miura and Tada, 2014). Similarly, SMM, through its role in sulfur metabolism, may contribute to the activation of sulfur-containing proteins essential for electron transport, such as ferredoxin and the cytochrome b6f complex (Tan et al., 2010; Haworth et al., 2017). Together, these mechanisms may explain the improvement in photosynthetic parameters despite the lack of significant changes in biomass-related traits.

In the first year, both biostimulants significantly enhanced transpiration, net CO_2 assimilation, and ΦPSII, while reducing NPQ in small-scale experiment. It should be noted that photosynthetic measurements at Göd were conducted one month after the first treatment during a distinct dry period, whereas at the large-scale site (Szarvas) they were measured later, just before harvest one month (see Materials and Methods, Section 2.3). This difference in timing complicates direct comparison between the two sites and may have contributed to the weaker or absent treatment effects observed at Szarvas. In the second year, no significant effects of the biostimulants were observed at either site. The reduced treatment effects observed in the second year may be attributed to interannual environmental variability, including differences in precipitation patterns and temperature conditions, with 2021 being notably drier than 2020 at both sites (see Materials and Methods). In addition, changes in soil nutrient availability over time may also have influenced plant responses. Furthermore, as a perennial species, Szarvasi-1 energy grass may exhibit cumulative physiological or morphological acclimation to repeated drought exposure, which could reduce its responsiveness to biostimulant treatments in subsequent years (Conrath et al., 2015). As a result, the relative impact of the treatments was smaller compared with the first year. Such differences in treatment response between years are consistent with previous reports, which indicate that the efficacy of plant biostimulants depends on both the severity of stress and the baseline resilience of the plants (Rouphael and Colla, 2020). In the large-scale experiment, the effects of treatment were generally weaker or absent, which may be attributed to environmental heterogeneity - such as variations in soil structure and composition, microclimate, and groundwater availability - leading to similar physiological performance between treated and control plants.

In addition to enhancing photosynthetic activity, SMM and NaSA treatments also tended to increase SOD and POD activities, although not all changes were statistically significant. These enzymes are key components of the antioxidant defence system, and similar responses have been reported under salt stress in wheat, a condition analogous to drought (Han et al., 2023). In the case of SMM, the trend of elevated POD activity appeared to be associated with enhanced lignin biosynthesis. This was supported by metabolomic and PCA analyses, which revealed increased levels of phenylalanine—a key precursor of lignin—as well as tyrosine, shikimic acid, and caffeic acid, intermediates of an alternative lignin biosynthetic route (Fig. 8). Together, these observations suggest a potential involvement of lignin-related metabolic processes in the stress response of SMM-treated plants, although no direct evidence of lignification was obtained in this study.

Both treatments also enhanced GR activity, an enzyme essential for regenerating reduced glutathione and maintaining redox homeostasis under drought stress (Madhu et al., 2022). By contrast, CAT and GPOX activities decreased in both years, which is atypical for drought stress but suggests that Szarvasi-1 plants may activate alternative antioxidant strategies when treated with NaSA or SMM (Mika et al., 2010; Ali et al., 2024).

APX activity showed a treatment-specific response: it significantly decreased in NaSA-treated plants but remained unchanged under SMM. Metabolomic analyses indicated reduced ascorbate levels in both treatments (Fig. 8), which may be associated with altered redox-related metabolic processes. PCA of the metabolomic data revealed distinct treatment-specific patterns: NaSA-treated plants were characterized by metabolic profiles consistent with increased osmoprotectant and flavonoid-related compounds, whereas SMM treatment was associated

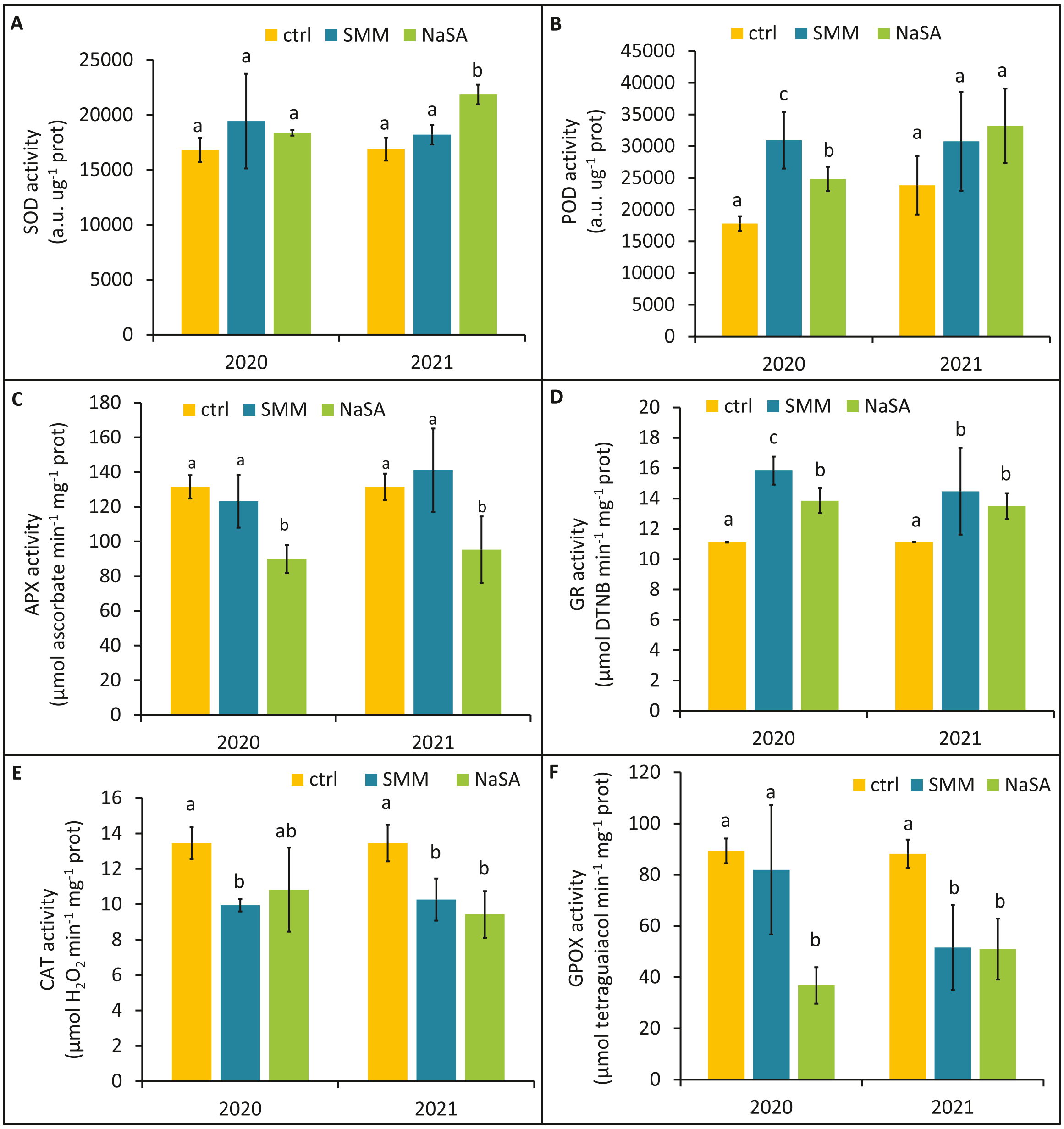

Fig. 6. Total superoxide dismutase (SOD: A), total class III peroxidase (POD: B), ascorbate peroxidase (APX: C), glutathione reductase (GR: D), catalase (CAT: E), and guaiacol peroxidase (GPOX: F) activities in the youngest fully developed leaves after the SMM and NaSA treatments in the small-scale experiment (in Göd) conducted on Szarvasi-1 energy grass plantations in 2020 and 2021. To compare differences among the treatments, one-way ANOVA was performed with Tukey-Kramer multiple comparisons post hoc test. Different lowercase letters indicate significant difference among the treatments ($p < 0.05$, $n = 9$). Error bars represent SD values. Statistical analyses were conducted separately for each year.

with metabolites linked to phenylpropanoid metabolism and lignin biosynthesis. This may therefore reflect its involvement in alternative metabolic processes. In particular, ascorbate may be utilized in pathways related to carbohydrate metabolism (e.g., ascorbate phosphate for sugar synthesis; Xiao et al., 2021) or flavonoid biosynthesis, where it serves as a cofactor for dioxygenases required for anthocyanin and flavonol formation (Smirnoff, 2000). PCA results support this interpretation, showing that NaSA treatment favored osmoprotectant and flavonoid production, whereas SMM treatment primarily promoted lignin biosynthesis.

Element analysis showed that SMM and NaSA treatments caused notable changes in element levels, such as potassium (K) and sodium (Na), in young plant tissues. Numerous studies have shown that K accumulation in both the vacuole and cytosol can enhance water uptake by improving osmotic adjustment (Mostofa et al., 2022; Mulet et al., 2023). Therefore, K is considered one of the most crucial osmolytes for plants under drought conditions. K levels increased significantly after treatment of Szarvasi-1 energy grass in the first year, aiding water uptake through osmotic adjustment. In the second year, K levels in treated and untreated plants were similar, with untreated plants already showing high K levels, likely due to their natural drought response. Thus, Szarvasi-1 energy grass appears capable of elevating K content without treatment, though biostimulants can provide short-term drought stress relief.

The overall levels of Na decreased, with significant differences between treated and untreated plants becoming evident in the second year. Lower Na levels help balance essential ions like K, aiding in enzyme activation and photosynthesis, while also maintaining osmotic pressure for proper cell function (Hussain et al., 2021). Therefore, the elevated K:Na ratio in treated plants was maintained by enhanced K uptake in the

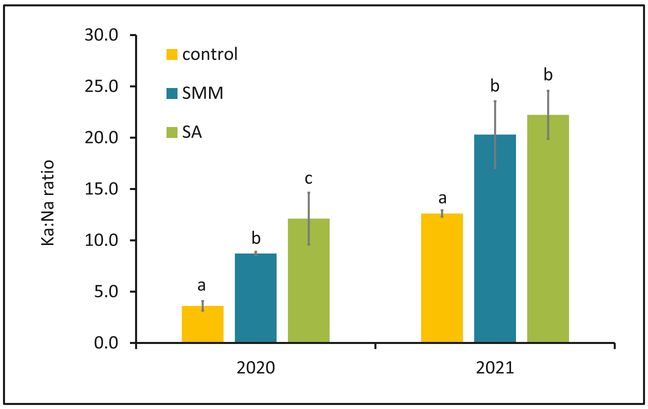

Fig. 7. The K to Na ratio in the youngest fully developed leaves of Szarvasi1 energy grass as affected by the SMM and NaSA treatments in the small-scale experiment (in Göd) conducted in 2020 and 2021. To compare differences among the treatments, one-way ANOVA was performed with Tukey-Kramer multiple comparisons post hoc test. Different lowercase letters indicate significant difference among the treatments ($p < 0.05$, $n = 7$). Error bars represent SD values. Statistical analyses were conducted separately for each year.

first year and by a more pronounced reduction in Na levels in the second year. This may be due to the plants activating mechanisms to exclude or sequester Na, such as the SOS1 plasma membrane Na^+/H^+ antiporter, which pumps excess Na out of the cells, reducing cytosolic Na toxicity (Xie et al., 2022). Additionally, the NHX1 tonoplast Na^+/H^+ antiporter plays a crucial role by transporting Na^+ into vacuoles, isolating it from the cytosol and thereby mitigating intracellular Na toxicity (Sharma et al., 2022). These mechanisms help the plants maintain ion balance and improve their stress tolerance which was also described in Szarvasi-1 energy grass (Arcoverde Cerveira Sterner et al., 2024). Moreover, the plants might have developed better potassium retention strategies, which could involve the regulation of K transporters and channels to optimize K uptake and retention, further supporting the observed change in the K:Na ratio (Farooq et al., 2021; Mostofa et al., 2022; Almeida et al., 2017). Methionine treatment in wheat under water deficit has been shown to maintain higher K levels while simultaneously reducing Na (Maqsood et al., 2022). This pattern is consistent with our observations in Szarvasi-1 energy grass. In rice under salt stress, exogenous SA application led to lower Na accumulation and higher K concentrations, thereby improving the K:Na ratio (Liu et al., 2022). Thus, both NaSA and SMM appear to modulate ion homeostasis through complementary mechanisms. On the one hand, NaSA (or SA-derived signalling) is proposed to influence H^+-ATPase (proton pump) activity,

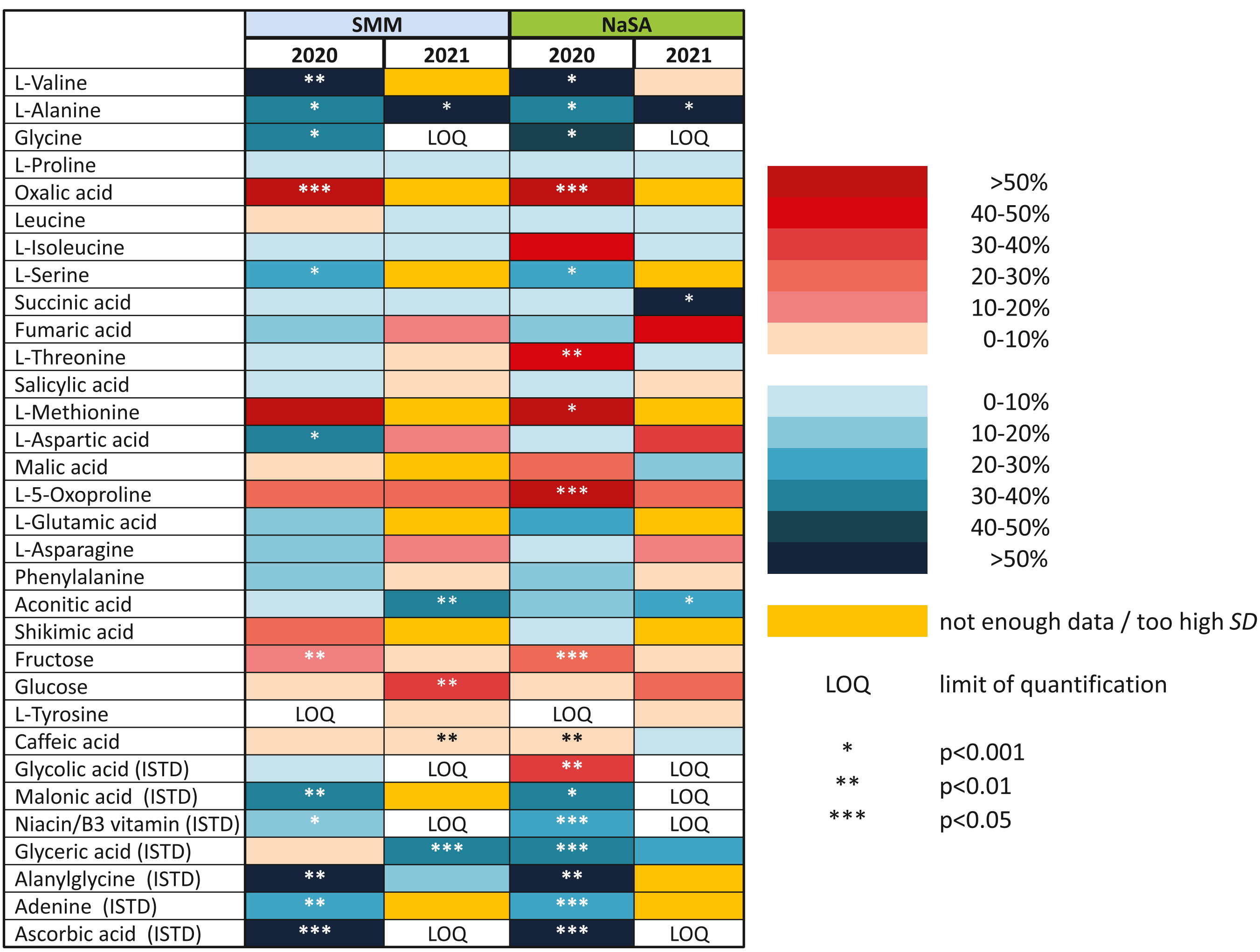

Fig. 8. Heat map of the metabolite content in the youngest fully developed leaves of Szarvasi-1 energy grass after SMM and NaSA treatments in the small-scale experiment (Göd, 2020–2021). Increases and decreases in metabolite content are shown in red and blue, respectively, with darker and lighter shades indicating the magnitude of change. Asterisks (*) denote statistically significant differences compared with the control, determined by one-way ANOVA followed by Tukey's post hoc test ($p < 0.05$, 0.01, or 0.001). "LOQ" indicates values below the limit of quantification. Statistical analysis was performed on mean values ($n = 3$–4). Changes in metabolite content in treated plants are expressed relative to the corresponding control plants (Supplementary Table S2).

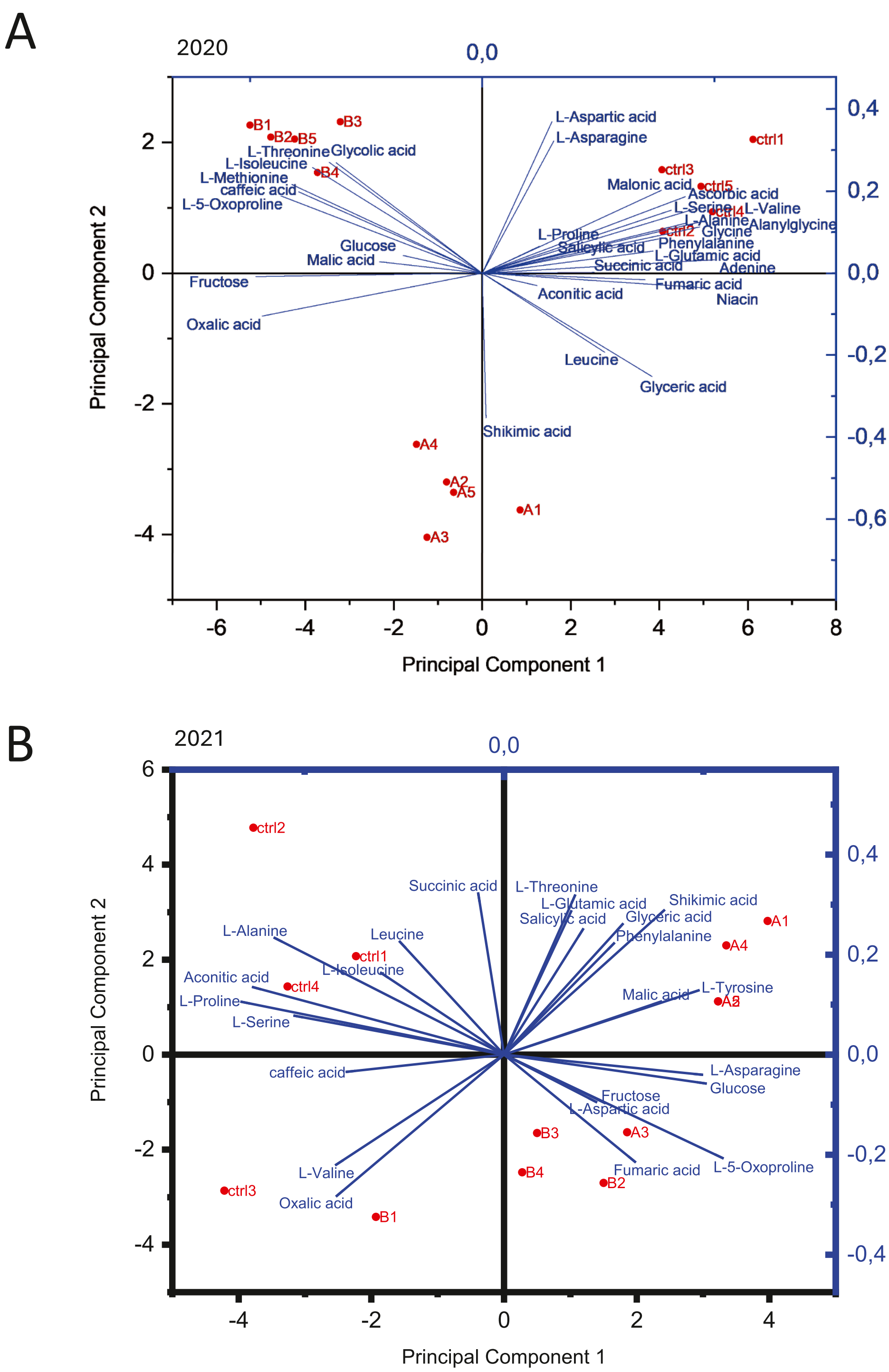

Fig. 9. PCA analysis of the changes in the metabolite composition in the youngest fully developed leaves of Szarvasi-1 energy grass measured after the SMM and NaSA treatments in the small-scale experiment (in Göd) conducted in 2020 (A) and 2021 (B). Groups represent the drought stressed untreated control plants (ctrl 1–4), SMM treated pplants (A1–4) and NaSA treated plants (B1–4). Positive correlations are indicated by vectors pointing in the same direction, while negative correlations are indicated by vectors pointing in opposite directions.

providing the proton motive force needed for K^+ uptake and Na^+ efflux, and to regulate expression of ion transporter genes such as HKT (high-affinity K^+/Na^+ transporters) and SOS1 to suppress Na uptake and favor K retention (see reviews on Na^+/K^+ homeostasis under salinity in Assaha et al., 2017). On the other hand, SMM—originating from methionine metabolism—not only contributes sulfur for synthesis of stress-related compounds (e.g. thiol-containing antioxidants, glutathione) but may also support the integrity or regulation of ion transport proteins or signalling pathways that enhance K retention and Na exclusion, although direct mechanistic studies are limited. In Szarvasi-1, prior work has shown that SMM treatments under heavy metal stress altered overall nutrient uptake patterns, including effects on potassium and iron (Rana et al., 2022) — indicating that SMM can influence ionic balance under stress.

Metabolomic profiling revealed treatment-associated changes in metabolic composition under SMM application. Elevated oxalic acid, glucose, and fructose levels are consistent with enhanced osmotic adjustment and ROS-related processes, with sugars likely contributing to osmoprotection in Szarvasi-1 energy grass (Sami et al., 2016; Zhang et al., 2024). In contrast, L-proline showed only minor changes, suggesting that soluble sugars may play a more prominent role than amino acids in osmotic adjustment under SMM treatment. L-methionine levels remained relatively stable, which may be related to exogenous SMM supply and its role in sulfur metabolism and associated defence processes (Rocha et al., 2020). Changes in secondary metabolism were also observed. In the first year, moderately elevated shikimic acid were consistent with changes in phenylpropanoid-related metabolism, while in the second year, more severe drought was accompanied by higher phenylalanine, tyrosine, and salicylic acid levels. These metabolites, which strongly contributed to the variance along PC2 are known to be involved in lignin and flavonoid biosynthesis, as well as in stress signalling and ROS detoxification. Together with the observed increase in POD activity, these patterns may indicate a shift toward enhanced defence-related metabolism. Concurrently, a general reduction in amino and organic acids (Kavi Kishor et al., 2015; Sharma et al., 2019) may reflect adjustments in central metabolism under stress conditions. Lower ascorbic acid content may reflect its role in additional metabolic pathways beyond direct antioxidative processes including carbohydrate metabolism (Xiao et al., 2021), while decreases in aconitic and malonic acids are consistent with reported alterations in TCA cycle intermediates under stress (Urano et al., 2009). Overall, these results suggest that SMM treatment is associated with metabolic adjustments that are consistent with enhanced osmotic regulation, antioxidant activity, and structural or defence-related processes. However, the specific pathways involved cannot be conclusively determined from the present data and would require further targeted investigation. NaSA treatment altered metabolic profiles under drought stress. Metabolomic analyses revealed increases in oxalic acid, glucose, fructose, L-methionine, and L-5-oxoproline, along with decreases in niacin and ascorbic acid (Fig. 8). Moderate increases in caffeic acid, glycolic acid, phenylalanine, tyrosine, shikimic acid, and salicylic acid were also detected, while malonic acid, alanylglycine, and adenine decreased. PCA analysis confirmed that NaSA-treated plants displayed a distinct metabolic profile compared to controls, consistent with enhanced osmoprotectant and secondary metabolite levels. While these data support treatment-specific metabolic shifts, interpretations regarding precise pathway mechanisms remain correlative as no direct enzymatic or molecular validation was performed. Nevertheless, the observed metabolite pattern aligns with the conclusion that NaSA promotes metabolic adjustments linked to stress adaptation rather than growth.

PCA analysis revealed distinct metabolic reorganizations under SMM and NaSA treatments, consistent with the observed enzymatic activity and metabolomic profile. In SMM-treated plants, shifts along PC2 were primarily associated with shikimic acid, glyceric acid, phenylalanine, L-tyrosine, malic acid, and salicylic acid, reflecting enhanced lignin and phenylpropanoid biosynthesis, ROS detoxification, and osmotic adjustment, in line with elevated POD activity and sugar levels. In NaSA-treated plants, prominent shifts along PC1 and to a lesser extent PC2 were associated with L-5-oxoproline, L-methionine, L-threonine, caffeic acid, glycolic acid, oxalic acid, and fumaric acid consistent with measured increases in sugars and other stress-related metabolites. Overall, the PCA results reflect the treatment-specific metabolic patterns observed: SMM-treated plants showed shifts associated with metabolites involved in lignin and phenylpropanoid pathways, osmotic adjustment, and ROS-related processes, whereas NaSA-treated plants exhibited shifts linked to sugars, amino acids, and other stress-related metabolites. These results are consistent with the observed enzymatic and metabolite changes and suggest differential metabolic responses under the two treatments.

5. Conclusions

Overall, the results indicate that SMM and NaSA trigger distinct but complementary stress acclimation strategies in Szarvasi-1 energy grass, involving structural reinforcement and metabolic adjustment, respectively. However, these responses primarily support stress tolerance rather than biomass production, highlighting a trade-off between growth and defence under drought conditions. The variability observed between years and experimental scales underscores the strong influence of environmental factors on biostimulant efficacy. Although the observed changes in metabolism, enzyme activity, and ion homeostasis are consistent with improved stress acclimation, the underlying regulatory mechanisms remain to be clarified. Future studies integrating molecular approaches and higher-resolution temporal sampling under controlled and field conditions would help to better resolve these processes and optimize the practical application of biostimulants in perennial energy crops.

Data availability

The data generated in the experiments are available from the corresponding author on reasonable request.

CRediT authorship contribution statement

Brigitta Müller: Writing – original draft, Visualization, Investigation, Formal analysis. **Kinga Benczúr:** Investigation. **Zoltán May:** Investigation. **Brigitta Tóth:** Investigation. **Paul Lopez:** Investigation. **Vitor Arcoverde Cerveira Sterner:** Investigation. **Gyula Sipos:** Supervision. **Csaba Gyuricza:** Supervision. **Gabriella Szalai:** Writing – review & editing, Supervision. **Ferenc Fodor:** Writing – review & editing, Project administration, Investigation, Funding acquisition, Conceptualization.

Declaration of competing interest

The authors declare that they have no known competing financial interests or personal relationships that could have appeared to influence the work reported in this paper.

Acknowledgements

This work was supported by the National Research, Development and Innovation Office of Hungary, [NKFIH K-132241] and by the European Structural and Investment Funds, [VEKOP-2.3.3–15–2016–00008].

Supplementary materials

Supplementary material associated with this article can be found, in the online version, at doi:10.1016/j.stress.2026.101389.

References

Aebi, H., 1984. Catalase in vitro. Meth. Enzym. 105, 121–126.

Ali, Q., Sami, A., Haider, M.Z., Ashfaq, M., Javed, M.A., 2024. Antioxidant production promotes defense mechanism and different gene expression level in *Zea mays* under abiotic stress. Sci. Rep. 14 (1), 7114.

Almeida, D.M., Oliveira, M.M., Saibo, N.J., 2017. Regulation of Na^+ and K^+ homeostasis in plants: towards improved salt stress tolerance in crop plants. Genet. Mol. Biol. 40 (1 suppl 1), 326–345.

Arcoverde Cerveira Sterner, V., Jobbágy, K., Tóth, B., Rudnóy, S., Sipos, G., Fodor, F., 2024. Increasing salinity sequentially induces salt tolerance responses in Szarvasi-1 energy grass. Plant Stress. 14, 100572.

Badr, A., Brüggemann, W., 2020. Comparative analysis of drought stress response of maize genotypes using chlorophyll fluorescence measurements and leaf relative water content. Photosynthetica 58 (2), 38–645.

Bandurska, H., 2022. Drought stress responses: coping strategy and resistance. Plants 11 (7), 922.
Bashir, S.S., Hussain, A., Hussain, S.J., Wani, O.A., Zahid Nabi, S., Dar, N.A., Mansoor, S., 2021. Plant drought stress tolerance: understanding its physiological, biochemical and molecular mechanisms. Biotechnol. Biotechnol. Equip. 35 (1), 1912–1925.
Batool, M., El-Badri, A.M., Hassan, M.U., Haiyun, Y., Chunyun, W., Zhenkun, Y., Zhou, G., 2022. Drought stress in Brassica napus: effects, tolerance mechanisms, and management strategies. J. Plant Growth Regul. 1–25.
Bouranis, D.L., Chorianopoulou, S.N., 2023. Foliar application of sulfur-containing compounds—pros and cons. Plants 12 (22), 3794.
Bradford, M., 1976. A rapid and sensitive method for the quantitation of microgram quantities of protein utilizing the principle of protein–dye binding. Anal. Biochem. 72, 248–254.
Ciria, C.S., Barro, R., Sanz, M., Ciria, P., 2020. Long-term yield and quality performance of perennial energy grasses (*Agropyron* spp.) on marginal land. Agronomy 10 (7), 1051.
Conrath, U., Beckers, G.J., Langenbach, C.J., Jaskiewicz, M.R., 2015. Priming for enhanced defense. Annu Rev. Phytopathol. 53 (1), 97–119.
Csete, S., Stranczinger, S., Szalontai, B., Farkas, A., Salamon-Albert, É., Kocsis, M., Vojtela, T., 2011. Tall wheatgrass cultivar Szarvasi-1 (*Elymus elongatus* Subsp. *Ponticus* cv. Szarvasi-1) as a potential energy crop for semi-arid lands of Eastern Europe. In: Nayeripour, M. (Ed.), Sustainable Growth and Applications in Renewable Energy Sources. IntechOpen, London, pp. 269–294.
de Araújo Silva, M.M., Ferreira, L.T., de Vasconcelos, F.M.T., Willadino, L., Camara, T.R., dos Santos, D.Y.A.C., de Oliveira, A.F.M., 2021. Water stress-induced responses in the growth, cuticular wax composition, chloroplast pigments and soluble protein content, and redox metabolism of two genotypes of *Ricinus communis* L. J. Plant Growth Regul. 40, 342–352.
Dietz, K.J., Zörb, C., Geilfus, C.M., 2021. Drought and crop yield. Plant Biol. 23 (6), 881–893.
Fariduddin, Q., Hayat, S., Ahmad, A., 2003. Salicylic acid influences net photosynthetic rate, carboxylation efficiency, nitrate reductase activity, and seed yield in *Brassica juncea*. Photosynthetica 41 (2), 281–284.
Farooq, M., Park, J.R., Jang, Y.H., Kim, E.G., Kim, K.M., 2021. Rice cultivars under salt stress show differential expression of genes related to the regulation of Na^+/K^+ balance. Front. Plant Sci. 12, 680131.
Giannapolitis, C.N., Ries, S.K., 1977. Superoxide dismutase. I. Occurrence in higher plants. Plant Physiol. 59, 309–314.
Gondor, O.K., Pál, M., Darkó, É., Janda, T., Szalai, G., 2016. Salicylic acid and sodium salicylate alleviate cadmium toxicity to different extents in maize (*Zea mays* L.). PLoS. One 11 (8), e0160157.
Gondor, O.K., Tajti, J., Hamow, K.Á., Majláth, I., Szalai, G., Janda, T., Pál, M., 2021. Polyamine metabolism under different light regimes in wheat. Int. J. Mol. Sci. 22.
Gupta, A., Rico-Medina, A., Caño-Delgado, A.I., 2020. The physiology of plant responses to drought. Science 368 (6488), 266–269.
Han, A., Wang, C., Li, J., Xu, L., Guo, X., Li, W., Liu, R., 2023. Physiological mechanism of sodium salicylate and folcisteine on alleviating salt stress in wheat seedlings. Sci. Rep. 13 (1), 22869.
Haworth, M., Catola, S., Marino, G., Brunetti, C., Michelozzi, M., Riggi, E., Centritto, M., 2017. Moderate drought stress induces increased foliar dimethylsulphoniopropionate (DMSP) concentration and isoprene emission in two contrasting ecotypes of Arundo donax. Front. Plant Sci. 8, 1016.
Hussain, S., Hussain, S., Ali, B., Ren, X., Chen, X., Li, Q., Ahmad, N., 2021. Recent progress in understanding salinity tolerance in plants: story of Na^+/K^+ balance and beyond. Plant Physiol. Biochem. 160, 239–256.
Kavi Kishor, P.B., Hima Kumari, P., Sunita, M.S.L., Sreenivasulu, N., 2015. Role of proline in cell wall synthesis and plant development and its implications in plant ontogeny. Front. Plant Sci. 6, 544.
Khan, M.I.R., Fatma, M., Per, T.S., Anjum, N.A., Khan, N.A., 2015. Salicylic acid-induced abiotic stress tolerance and underlying mechanisms in plants. Front. Plant Sci. 6, 462.
Khalvandi, M., Siosemardeh, A., Roohi, E., Keramati, S., 2021. Salicylic acid alleviated the effect of drought stress on photosynthetic characteristics and leaf protein pattern in winter wheat. Heliyon 7 (1).
Klessig, D.F., Tian, M., Choi, H.W., 2016. Multiple targets of salicylic acid and its derivatives in plants and animals. Front. Immunol. 7, 206.
Konieczny, R., Banaś, A.K., Surówka, E., Michalec, Ż., Miszalski, Z., Libik-Konieczny, M., 2014. Pattern of antioxidant enzyme activities and hydrogen peroxide content during developmental stages of rhizogenesis from hypocotyl explants of *mesembryanthemum crystallinum* L. Plant Cell Rep. 33, 165–177.
Laemmli, U.K., 1970. Cleavage of structural proteins during the assembly of the head of bacteriophage T4. Nature 227 (5259), 680–685.
Li, S., Li, X., Wei, Z., Liu, F., 2020. ABA-mediated modulation of elevated CO_2 on stomatal response to drought. Curr. Opin. Plant Biol. 56, 174–180.
Liu, Z., Ma, C., Hou, L., Wu, X., Wang, D., Zhang, L., Liu, P., 2022. Exogenous SA affects rice seed germination under salt stress by regulating Na^+/K^+ balance and endogenous GAs and ABA homeostasis. Int. J. Mol. Sci. 23 (6), 3293.
Lourkisti, R., Froelicher, Y., Morillon, R., Berti, L., Santini, J., 2022. Enhanced photosynthetic capacity, osmotic adjustment and antioxidant defenses contribute to improve tolerance to moderate water deficit and recovery of triploid citrus genotypes. Antioxidants 11 (3), 562.
Ludmerszki, E., Paldi, K., Racz, I., Szigeti, Z., Rudnoy, S.Z., 2014. The promising role of exogenous S-methylmethionine in agriculture, in the case of maize cultivation. Appl. Ecol. Environ. Res. 12, 777–785.
Madhu Kaur, A., Tyagi, S., Shumayla Singh, K., Upadhyay, S.K, 2022. Exploration of glutathione reductase for abiotic stress response in bread wheat (*Triticum aestivum* L.). Plant Cell Rep. 41 (3), 639–654.
Maqsood, M.F., Shahbaz, M., Kanwal, S., Kaleem, M., Shah, S.M.R., Luqman, M., Farhat, F., 2022. Methionine promotes the growth and yield of wheat under water deficit conditions by regulating the antioxidant enzymes, reactive oxygen species, and ions. Life 12 (7), 969.
Mika, A., Boenisch, M.J., Hopff, D., Lüthje, S., 2010. Membrane-bound guaiacol peroxidases from maize (Zea mays L.) roots are regulated by methyl jasmonate, salicylic acid, and pathogen elicitors. J. Exp. Bot. 61 (3), 831–841.
Miura, K., Tada, Y., 2014. Regulation of water, salinity, and cold stress responses by salicylic acid. Front. Plant Sci. 5, 4.
Mohamed, H.I., El-Shazly, H.H., Badr, A., 2020. Role of salicylic acid in biotic and abiotic stress tolerance in plants. Plant Phenolics. Sustain. Agric. 1, 533–554. *Volume*.
Mostofa, M.G., Rahman, M.M., Ghosh, T.K., Kabir, A.H., Abdelrahman, M., Khan, M.A.R., Tran, L.S.P., 2022. Potassium in plant physiological adaptation to abiotic stresses. Plant Physiol. Biochem. 186, 279–289.
Mulet, J.M., Porcel, R., Yenush, L., 2023. Modulation of potassium transport to increase abiotic stress tolerance in plants. J. Exp. Bot. 74 (19), 5989–6005.
Müller, B., Arcoverde Cerveira Sterner, V., Papp, L., May, Z., Orlóci, L., Gyuricza, C., Fodor, F., 2022. Alkaline salt tolerance of the biomass plant Arundo donax. Agronomy 12 (7), 1589.
Nakano, Y., Asada, K., 1981. Hydrogen peroxide is scavenged by ascorbate-specific peroxidase in spinach chloroplasts. Plant Cell Physiol. 22 (5), 867–880.
Ogawa, S., Mitsuya, S., 2012. S-methylmethionine is involved in the salinity tolerance of Arabidopsis thaliana plants at germination and early growth stages. Physiol. Plant 144 (1), 13–19.
Ozturk, M., Turkyilmaz Unal, B., García-Caparrós, P., Khursheed, A., Gul, A., Hasanuzzaman, M., 2021. Osmoregulation and its actions during the drought stress in plants. Physiol. Plant 172 (2), 1321–1335.
Pallas, B., Clément-Vidal, A., Rebolledo, M.C., Soulié, J.C., Luquet, D., 2013. Using plant growth modeling to analyze C source–sink relations under drought: inter-and intraspecific comparison. Front. Plant Sci. 4, 437.
Pamungkas, S.S.T., Farid, N., 2022. Drought stress: responses and mechanism in plants. Rev. Agric. Sci. 10, 168–185.
Pirasteh-Anosheh, H., Ranjbar, G., Hasanuzzaman, M., Khanna, K., Bhardwaj, R., Ahmad, P., 2022. Salicylic acid-mediated regulation of morpho-physiological and yield attributes of wheat and barley plants in deferring salinity stress. J. Plant Growth Regul. 41 (3), 1291–1303.
Rana, D., Arcoverde Cerveira Sterner, V., May, Z., Sipos, G., Fodor, F., 2025. Combined metal treatments cause marked changes in the ionomic patterns in Szarvasi-1 energy grass shoot biomass. Plant Soil. 1–19.
Rana, D., Arcoverde Cerveira Sterner, V., Potluri, A.K., May, Z., Müller, B., Solti, Á., Rudnóy, S., Sipos, G., Gyuricza, C., Fodor, F., 2022. S-methylmethionine effectively alleviates stress in Szarvasi-1 energy grass by reducing root-to-shoot cadmium translocation. Plants 11, 2979.
Rév, A., Tóth, B., Solti, Á., Sipos, G., Fodor, F., 2017. Responses of Szarvasi-1 energy grass to sewage sludge treatments in hydroponics. Plant Physiol. Biochem. 118, 627–633.
Rocha, P.S., Machado, F.B., Arenhart, R.A., Margis-Pinheiro, M., 2020. Functional and evolutionary insights into plant methionine metabolism. Biol. Res. 53 (1), 1–14.
Rodrigues, J., Inzé, D., Nelissen, H., Saibo, N.J., 2019. Source–sink regulation in crops under water deficit. Trends. Plant Sci. 24 (7), 652–663.
Rouphael, Y., Colla, G., 2020. Biostimulants in agriculture. Front. Plant Sci. 11, 40.
Sami, F., Yusuf, M., Faizan, M., Faraz, A., Hayat, S., 2016. Role of sugars under abiotic stress. Plant Physiol. Biochem. 109, 54–61.
Seleiman, M.F., Al-Suhaibani, N., Ali, N., Akmal, M., Alotaibi, M., Refay, Y., Battaglia, M. L., 2021. Drought stress impacts on plants and different approaches to alleviate its adverse effects. Plants 10 (2), 259.
Sharma, A., Shahzad, B., Rehman, A., Bhardwaj, R., Landi, M., Zheng, B., 2019. Response of phenylpropanoid pathway and the role of polyphenols in plants under abiotic stress. Molecules 24 (13), 2452.
Sharma, H., Sharma, A., Sidhu, S., Upadhyay, S.K., 2022. Na+/H+ antiporter (NHX) and salt stress tolerance. Cation Transporters in Plants. Academic Press, pp. 99–113.
Shemi, R., Wang, R., Gheith, E.S.M., Hussain, H.A., Hussain, S., Irfan, M., Wang, L., 2021. Effects of salicylic acid, zinc and glycine betaine on morpho-physiological growth and yield of maize under drought stress. Sci. Rep. 11 (1), 3195.
Singh, M., Kumar, J., Singh, S., Singh, V.P., Prasad, S.M., 2015. Roles of osmoprotectants in improving salinity and drought tolerance in plants: a review. Rev. Environ. Sci. Bio Technol. 14, 407–426.
Sipos, G., Solti, Á., Czech, V., Vashegyi, I., Tóth, B., Cseh, E., Fodor, F., 2013. Heavy metal accumulation and tolerance of energy grass (Elymus elongatus subsp. ponticus cv. Szarvasi-1) grown in hydroponic culture. Plant Physiol. Biochem. 68, 96–103.
Smirnoff, N., 2000. Ascorbate biosynthesis and function in photoprotection. Philos. Trans. R. Soc. Lond. B Biol. Sci. 355 (1402), 1455–1464.
Smith, I.K., Vierheller, T.L., Thorne, C.A., 1988. Assay of glutathione reductase in crude tissue homogenates using 5,50 -dithiobis (2-nitrobenzoic acid). Anal. Biochem. 175, 408–413.
Sohag, A.A.M., Tahjib-Ul-Arif, M.D., Brestic, M., Afrin, S., Sakil, M.A., Hossain, M.T., Hossain, M.A., 2020. Exogenous salicylic acid and hydrogen peroxide attenuate drought stress in rice. Plant Soil Environ. 66 (1), 7–13.
Solórzano, E., Corpas, F.J., González-Gordo, S., Palma, J.M., 2020. Reactive oxygen species (ROS) metabolism and nitric oxide (NO) content in roots and shoots of rice (Oryza sativa L.) plants under arsenic-induced stress. Agronomy 10 (7), 1014.
Song, W., Shao, H., Zheng, A., Zhao, L., Xu, Y., 2023. Advances in roles of salicylic acid in plant tolerance responses to biotic and abiotic stresses. Plants 12 (19), 3475.

Sterner, V.A.C., Jobbágy, K., Tóth, B., Rudnóy, S., Sipos, G., Fodor, F., 2024. Increasing salinity sequentially induces salt tolerance responses in Szarvasi-1 energy grass. Plant. Stress. 14, 100572.
Tan, Q., Zhang, L., Grant, J., Cooper, P., Tegeder, M., 2010. Increased phloem transport of S-methylmethionine positively affects sulfur and nitrogen metabolism and seed development in pea plants. Plant Physiol. 154 (4), 1886–1896.
Urano, K., Maruyama, K., Ogata, Y., Morishita, Y., Takeda, M., Sakurai, N., Shinozaki, K., 2009. Characterization of the ABA-regulated global responses to dehydration in Arabidopsis by metabolomics. Plant J. 57 (6), 1065–1078.
Xiao, M., Li, Z., Zhu, L., Wang, J., Zhang, B., Zheng, F., Zhang, Z., 2021. The multiple roles of ascorbate in the abiotic stress response of plants: antioxidant, cofactor, and regulator. Front. Plant Sci. 12, 598173.
Xie, Q., Zhou, Y., Jiang, X., 2022. Structure, function, and regulation of the plasma membrane Na+/H+ antiporter salt overly sensitive 1 in plants. Front. Plant Sci. 13, 866265.
Xin, K., Wu, Y., Ikram, A.U., Jin, Y., Liu, S., Zhang, Y., Chen, J., 2024. Salicylic acid cooperates with different small molecules to control biotic and abiotic stress responses. J. Plant Physiol., 154406
Yadav, B., Jogawat, A., Rahman, M.S., Narayan, O.P., 2021. Secondary metabolites in the drought stress tolerance of crop plants: a review. Gene Rep. 23, 101040.
Yang, L., Wang, X., Zhao, F., Zhang, X., Li, W., Huang, J., Yang, D., 2023. Roles of S-adenosylmethionine and its derivatives in salt tolerance of cotton. Int. J. Mol. Sci. 24 (11), 9517.
Zahra, N., Hafeez, M.B., Kausar, A., Al Zeidi, M., Asekova, S., Siddique, K.H., Farooq, M., 2023. Plant photosynthetic responses under drought stress: effects and management. J. Agron. Crop. Sci. 209 (5), 651–672.
Zhang, X.J., Wu, C., Liu, B.Y., Liang, H.L., Wang, M.L., Li, H., 2024. Transcriptomic and metabolomic profiling reveals the drought tolerance mechanism of Illicium difengpi (Schisandraceae). Front. Plant Sci. 14, 1284135.